

# Ultrafast dynamics of excited state in oxy-hemoglobin

Takayoshi Kobayashi<sup>1,2,3,4\*</sup> and Atsushi Yabushita<sup>2</sup>

<sup>1</sup>Department of Applied Physics and Chemistry and Institute for Laser Science, University of Electro-Communications, 1-5-1 Chofugaoka, Chofu 182-8585, Japan

<sup>2</sup>Department of Electrophysics, National Chiao-Tung University, Hsinchu 300, China

<sup>3</sup>ICORP, JST, 4-1-8 Honcho, Kawaguchi, Saitama 332-0012, Japan

<sup>4</sup>Institute of Laser Engineering, Osaka University, 2-6 Yamada-oka, Suita, Osaka 565-0971, Japan

\*Corresponding author: kobayashi@ils.uec.ac.jp

Received December 10, 2010; accepted January 13, 2011; posted online June 29, 2011

We perform ultrafast transient absorption spectroscopy of oxy-hemoglobin by a pump-probe method with ultrashort laser pulses. Negative time-range of the observed traces, where the pump pulse precedes the probe pulse, is analyzed to study the electronic coherence dynamics between the excited state and the ground state, and the vibrational coherence in the electronic excited state. The analysis result shows that the electronic coherence between the electronic ground state and the Q-band state dephases in  $45 \pm 5$  fs. The vibrational dephasing times of modes with frequencies of 210, 393, 554, 731, and  $1106 \text{ cm}^{-1}$  are found to be 449, 366, 555, 1085, and  $>1330$  fs, respectively.

OCIS codes: 320.7150, 320.7100, 320.2250, 300.6530, 160.1435.

doi: 10.3788/COL201109.S10605.

Heme protein was studied by many research groups for decades because of its extreme biological importance in the mechanism of oxygen transfer<sup>[1–7]</sup>. Previous studies have demonstrated that heme photophysics is similar in hemoglobin (Hb), heme proteins, and heme model systems<sup>[8–12]</sup>. All these hemes exhibit two excited states, designated as  $\text{Hb}^*_{\text{I}}$  and  $\text{Hb}^*_{\text{II}}$ . Data shows that  $\text{Hb}^*_{\text{I}}$  is formed in less than 50 fs and then decays to form  $\text{Hb}^*_{\text{II}}$  in 300 fs. The lifetime of the  $\text{Hb}^*_{\text{II}}$  electronic state is roughly 3 ps, followed by the recovery of the ground state. This electronic relaxation is sufficiently rapid such that the intra-molecular vibrational redistribution (IVR) and the vibrational cooling occur on a similar (or even slightly longer) time scale. In our previous work,  $\text{Hb}^*_{\text{I}}$  formation after the excitation of oxy-Hb was time-resolved for the first time to be  $45 \pm 5$  fs. Both photo-dissociation and heme-iron movement out of plane were also found to occur very rapidly ( $<50$  fs) in order to create a species that resembled deoxy-Hb.  $\text{Hb}^*_{\text{I}}$  transient spectra appeared on the same time scale as photolysis in both  $\text{Hb}^*_{\text{CO}}$  and  $\text{Hb}^*_{\text{NO}}$ <sup>[12]</sup>.

As shown in a previous study<sup>[13]</sup>, the absorption spectrum of Hb in a visible spectral region (Q-band) has two peaks for oxy-Hb and only one peak for deoxy-Hb. Therefore, the time-resolved spectroscopy in the visible spectral region is expected to observe spectral change reflecting the ultrafast photodissociation of oxyhemoglobin. In the present letter, we estimate the decay time of electronic coherence between the linear combination of the ground state and the Q-band electronic state. Vibrational dephasing times are also determined.

Hemoglobin from bovine blood (Sigma-Aldrich) was dissolved in water with a phosphate buffer stabilized at pH 7.7. The sample solution had an optical density of about 1.0 at 540 nm in a 1-mm cell (6210-27501, GL Science) used for femtosecond pump-probe experiment. A Ti:sapphire multi-pass amplifier was used to generate second harmonics and a visible broadband spectrum was used as the pump pulse and the probe pulse, respectively, in the pump-probe measurement. Pump-probe

signals were detected with a 128-channel lock-in amplifier scanning delay by a motorized stage at 1-fs step. All measurements were performed at room temperature ( $294 \pm 1$  K).

The laser spectrum and absorption spectrum of the oxy-hemoglobin solution sample are shown in Fig. 1. The spectral overlap between the laser and the sample absorption is very good. The laser spectrum is composed of a main peak at  $17500 \text{ cm}^{-1}$ , a weak peak around  $14500 \text{ cm}^{-1}$ , and a shoulder at about  $16000 \text{ cm}^{-1}$ . The absorption spectrum has two clearly separated peaks around  $18550$  and  $17300 \text{ cm}^{-1}$ , which are attributed to Q(00) and Q(10), respectively. The peak locations are in agreement with those in literature<sup>[13]</sup>.

The probe delay time dependence of the absorbance change probed at 556, 588, 617, 653, and 685 nm in the observation time ranged from  $-70$  to 1900 fs is shown in Fig. 2(a). The sample is first excited to the  $S_2$  state (the Soret band of heme) by the 395-nm pump pulse. The positive signal of the absorbance change observed in the visible region of Fig. 2(a) is probably the excited-state absorption from  $S_2$  state to a higher-lying excited state. Figure 2(b) shows the Fourier power spectra of the to 430 fs. In our previous work<sup>[14]</sup>, we classified the

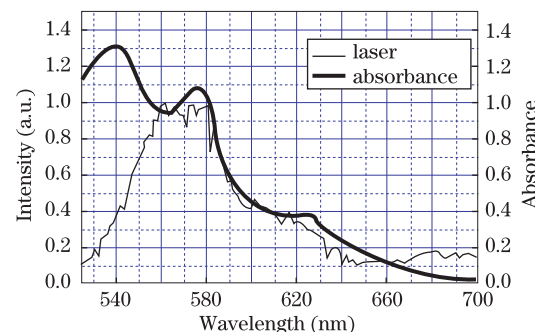


Fig. 1. Laser spectrum (thin line) and absorption spectrum (thick line) of oxy-hemoglobin solution sample.

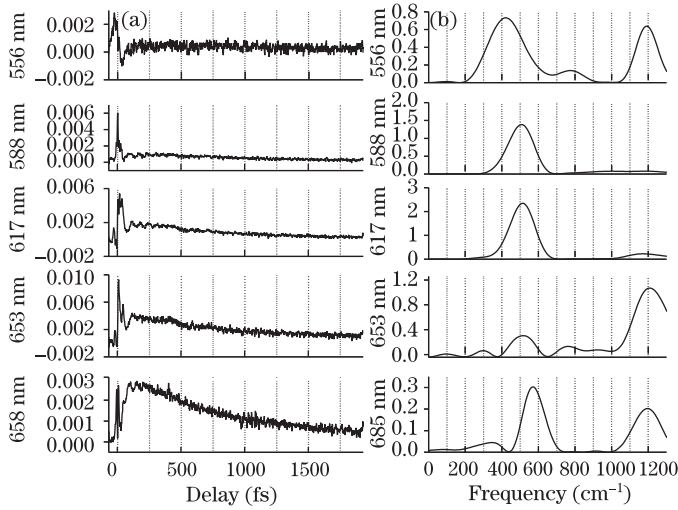


Fig. 2. (a) Several real-time traces of different absorbance and (b) their Fourier power spectra at 556, 588, 617, 653, and 685 nm in the probe delay time range extending from  $-70$  fs up to 1930 fs.

dynamic vibronic couplings in vibrational real-time spectra. Discussion on probe wavelength dependence of the Fourier power spectra is left to a future study after the vibrational phases of molecular vibrations are observed at a higher signal-to-noise ratio.

In Ref. [12], Petrich *et al.* performed the time-resolved absorption measurement of hemoglobin, myoglobin, and protoheme, both unligated and ligated with diatomic molecules. The spectral range was near ultraviolet (UV) and blue spectral between 400 and 490 nm. In the study, the absorbance change observed for  $\text{HbO}_2$  at 414 nm was found to be

$$\Delta A(t) = \Delta A'_1 \exp(-t/\tau'_1) + \Delta A'_2 \exp(-t/\tau'_2) + \Delta A'_3 \exp(-t/\tau'_3) + \Delta A'_4 \exp(-t/\tau'_4), \quad (1)$$

where the time constants of  $\tau'_1$ ,  $\tau'_2$ ,  $\tau'_3$ , and  $\tau'_4$  were determined to be  $<50$  fs, 300 fs, 2.5 ps, and  $\gg 10$  ps, respectively. The time constants obtained in the present study are considered to be corresponding to those obtained in the previous study, in such a way that  $\tau_1 = \tau'_1$ ,  $\tau_2$  is obtained from the mixed contribution of components of  $\tau'_2$  and  $\tau'_3$ , and  $\tau_3$  is the remaining part. The present measurement up to 1.9 ps does not allow us to obtain the time constant of 2.5 ps causing a mixture between  $\tau'_2$  and  $\tau'_3$ .

In real-time traces observed in the full range of probe photon energy, there exist unexpectedly finite-size signals which apparently violate causality. The signal intensities decrease with increasing negative delay time, and they almost completely disappear at the delay of about  $-70$  fs. This can be explained as follows.

On pump probe measurement, unperturbed population differences occur because the presence of the pump field modifies the other free decay of the probe-induced polarization (called perturbed free induction decay term). It persists when the probe precedes the pump, and rises with the time constant  $T_2$ . The signal in the negative time range is discussed in terms of the perturbed free induction decay.

A coherent artifact generated by the buffer solution stored in the 1-mm-thick glass cell is shown in Fig. 3(a).

The signal is averaged over the probe wavelength from 573 to 586 nm (i.e., near the peak of the probe spectrum) where the coherent artifact is observed with high intensity. It demonstrates that the artifact can modify the shape of time traces between  $-10$  and 10 fs.

The real-time trace of absorbance change integrated over the spectral range from 552 to 571 nm and the single exponential fitted decay function in negative delay time region are studied. The fitting result is plotted in Fig. 3(b). From the analysis, the electronic dephasing time is thus obtained to be  $T_2 = 25 \pm 2$  fs. In the rate of dephasing ( $1/T_2$ ) obtained from the plots, three components are given below:

$$\frac{1}{T_2} = \frac{1}{2T_1} + \frac{1}{T'_2} + \frac{1}{T_2^*}, \quad (2)$$

where  $T_1$  is the population decay time, and  $T'_2$  and  $T_2^*$  are electronic pure dephasing time and phase relaxation time due to inhomogeneous broadening, respectively. The short population decay time  $T_1 = \tau_1 = 45$  fs of excited state lifetime, which corresponds to  $\text{Hb}^*_1$  formation after the excitation of oxy-hemoglobin, is determined from real-time traces in the positive delay time range as described in the previous section. Then from  $T_2 = 25 \pm 2$  fs and  $T_1 = \tau_1 = 45$  fs,  $(1/T'_2 + 1/T_2^*)^{-1} = 34.6$  fs is obtained.

Therefore the upper limit of both the two time constants,  $T'_2$  and  $T_2^*$ , is 34.6 fs. To discuss absolute value of pure phase relaxation time constant  $T'_2$ , we must have the information of  $T_2^*$ . However, since it is difficult to determine the value, discussion is to be made here using the upper limit of the value.

The absorption spectrum has two clearly separated peaks around 18550 and 17300  $\text{cm}^{-1}$ , which are attributed to Q(00) and Q(10), respectively (see Fig. 1). The inhomogeneous broadening is then expected to be small enough to resolve the two vibrational peaks. This indicates that the phase relaxation time is substantially longer than the molecular vibrational period of 26.7 fs,

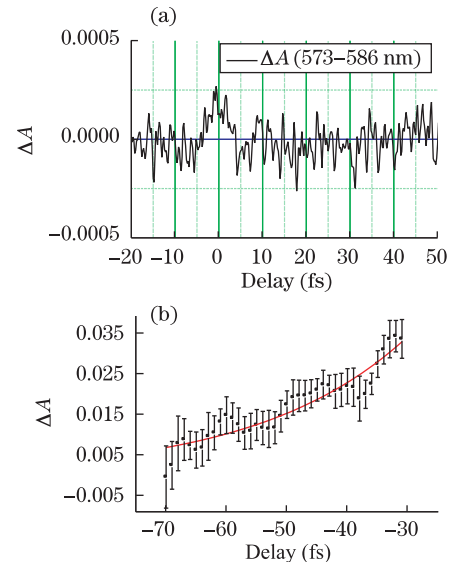


Fig. 3. (a) Coherent artifact generated by the buffer solution stored in a 1-mm-thick glass cell. (b) Real-time trace (thin curve) of absorbance change integrated over the spectral range from 552 to 571 nm and a single exponential function (thick curve) fitted in the negative delay time region.

**Table 1. Peak Frequencies of Fourier Power Spectra of the Oscillating Components of Real-time Traces in the Positive and Negative Time Ranges**

	Frequency ( $\text{cm}^{-1}$ )	Width ( $\text{cm}^{-1}$ )	Lifetime (fs)	Assignment
Negative Time Range	1254	782	26	$\delta(\text{C}_m\text{H})$
	210	69	449	$\nu(\text{Fe-His})$
Positive Time Range	393	74	336	$\delta(\text{C-CH}_3)$
	554	65	555	$\nu(\text{Fe-O}_2)$
	731	57	1085	$\nu(\text{pyr breathing})$
	1106	44	>1300	$\nu(\text{C}_\beta\text{-methyl})$

which corresponds to the  $1250\text{ cm}^{-1}$  frequency of the vibrational structure. Therefore, together with the upper limit value of 34.6 fs, it can be safely assumed that  $T_2^*$  is much longer than the period. Then  $T_2'$  is determined to be about 35 fs. Therefore, about 72% of the phase decay is due to pure dephasing process and 28% is due to population decay associated with the electronic relaxation which is, in turn, associated with extremely fast photo-dissociation. Such a short pure dephasing time may indicate that the preceding sign of ultrafast photo-dissociation is taking place in the electronic coherence of electronic excited state of the hemoglobin molecule. The effect of inhomogeneity is also relatively small and estimated to be smaller than about 10% of the electronic phase relaxation.

In conclusion, by utilizing data in a negative time-range of ultrafast pump-probe spectroscopy where pump pulse precedes probe pulse, we study the dynamics of electronic coherence between the electronic excited state and the electronic ground state, and that of vibrational coherence in an electronic excited state. The dephasing time of electronic coherence composed by the linear combination of the ground state and the Q-band electronic state is determined to be  $45\pm 5$  fs. Vibrational dephasing times of modes with frequencies of 210, 393, 554, 731, and  $1106\text{ cm}^{-1}$  are found to be 449, 366, 555, 1085, and >1330 fs, respectively.

This work was supported by the International Cooperative Research Project (ICORP) Program of the Japan Science and Technology Agency, the National Science Council, Taiwan, China (No. NSC 98-2112-M-009-001-MY3), a grant from the Ministry of Education, Aiming for Top University Program at National Chiao-Tung University, a Grant-in-Aid for Scientific Research from the Japan Society for the Promotion of Science (No. JSPS-GASR-14002003).

## References

1. M. F. Perutz, W. Bolton, R. Diamond, H. Muirhead, and H. C. Watson, *Nature* **203**, 687 (1964).
2. H. Muirhead, J. Cox, L. Mazzarella, and M. F. Perutz, *J. Chim. Phys.* **65**, 188 (1968).
3. S. Franzen, B. Bohn, C. Poyart, G. Depillis, S. G. Boxer, and J. L. Martin, *J. Biol. Chem.* **270**, 1718 (1995).
4. D. G. Lambright, S. Balasubramanian, and S. G. Boxer, *Chem. Phys.* **158**, 249 (1991).
5. S. Franzen and S. G. Boxer, *J. Biol. Chem.* **272**, 9655 (1997).
6. S. Franzen, J. C. Lambry, B. Bohn, C. Poyart, and J. L. Martin, *Nature Struct. Biol.* **1**, 230 (1994).
7. E. H. Harutyunyan, T. N. Safonova, I. P. Kuranova, A. N. Popov, A. V. Teplyakov, G. V. Obmolova, A. A. Rusakov, B. K. Vainshtein, G. G. Dodson, J. C. Wilson, and M. F. Perutz, *J. Mol. Biol.* **251**, 104 (1995).
8. J. M. Baldwin and C. Chothia, *J. Mol. Biol.* **129**, 175 (1979).
9. S. Franzen, B. Bohn, C. Poyart, and J. L. Martin, *Biochemistry* **34**, 1224 (1995).
10. J. L. Martin, A. Migus, C. Poyart, Y. Lecarpentier, R. Astier, and A. Antonetti, *Proc. Natl. Acad. Sci. U.S.A.* **80**, 173 (1983).
11. M. F. Perutz, *Annu. Rev. Biochem.* **48**, 327 (1979).
12. J. W. Petrich, C. Poyart, and J. L. Martin, *Biochemistry* **27**, 4049 (1988).
13. R. R. Anderson and A. Parrish, *J. Invest. Dermatol.* **77**, 13 (1981).
14. T. Kobayashi, J. Du, W. Feng, and K. Yoshino, *Phys. Rev. Lett.* **101**, 037402 (2008).